The Journal of Experimental Biology 210, 2333-2345
Published by The Company of Biologists 2007
doi:10.1242/jeb.004457

Variations in motor unit recruitment patterns occur within and between muscles in the running rat (*Rattus norvegicus*)

E. F. Hodson-Tole* and J. M. Wakeling

The Structure and Motion Laboratory, The Royal Veterinary College, Hawkshead Lane, North Mymms, Hatfield, Hertfordshire, AL9 7TA, UK

*Author for correspondence (e-mail: etole@rvc.ac.uk)

Accepted 18 April 2007

Summary

Motor units are generally considered to follow a set, orderly pattern of recruitment within each muscle with activation occurring in the slowest through to the fastest units. A growing body of evidence, however, suggests that recruitment patterns may not always follow such an orderly sequence. Here we investigate whether motor unit recruitment patterns vary within and between the ankle extensor muscles of the rat running at 40 cm s^{-1} on a level treadmill. In the past it has been difficult to quantify motor unit recruitment patterns during locomotion; however, recent application of wavelet analysis techniques has made such detailed analysis of motor unit recruitment possible. Here we present methods for quantifying the interplay of fast and slow motor unit recruitment based on their myoelectric signals. Myoelectric data were collected from soleus, plantaris and medial gastrocnemius muscles representing populations of slow, mixed and fast fibres, respectively, and providing a good opportunity to relate myoelectric frequency content to motor unit recruitment patterns. Following wavelet transformation, principal component analysis quantified signal intensity and relative frequency content. Significant differences in signal frequency content occurred between different time points within a stride ($P<0.001$). We optimised high- and low-frequency wavelets to the major signals from the fast and slow motor units. The goodness-of-fit of the optimised wavelets to the signal intensity was high for all three muscles ($r^2>0.98$). The low-frequency band had a significantly better fit to signals from the soleus muscle ($P<0.001$), while the high-frequency band had a significantly better fit to the medial gastrocnemius ($P<0.001$).

Key words: fibre-type, frequency band analysis, muscle, principal component, wavelet, EMG.

Introduction

The basic functional unit of the neuromuscular system is the motor unit, which is defined as a motoneuron and all the muscle fibres that it innervates (Henneman and Olson, 1965). The metabolic and mechanical properties of motor units have been extensively researched and a number of classification systems have been developed based on physiology (Burke et al., 1973), metabolism (Peter et al., 1972) and myosin heavy chain profile (Schiaffino et al., 1989). Due to variation in sarcomere structure and organisation, differences exist in the mechanical properties of different muscle fibres (Hill, 1950; Johnston, 1991). Most vertebrate muscles contain a mixture of muscle fibre types, which are proposed to act like a gearing system, facilitating effective movement over a wide range of speeds and loads. Through studying stretch reflexes in decerebrate cats it has been found that, as activation stimulus increases, successively faster muscle fibres are recruited in an orderly fashion, termed the 'size principle' (Henneman et al., 1965a; Henneman et al., 1965b). This indicates that slow fibres are used to power slow and medium speed movements, with both slow and fast fibres being used to power more rapid movements. There are many examples where the size principle has been shown to hold true and its predictions have formed a corner stone in current understanding of muscle function for many years. A growing body of evidence, however, suggests that it may not be appropriate to assume that this principle adequately describes motor unit recruitment in all situations (Wakeling, 2005). Comparing activity across different muscles has shown that during the paw-shake in the cat (Smith et al., 1980), fast walking in cats (Prilutsky et al., 1996) and swimming in the blue gilled sunfish (Jayne and Lauder, 1994), faster muscles are selectively used for faster tasks. It is therefore possible that, within a mixed fibre muscle, selective recruitment of appropriate fibre types may occur. Glycogen depletion studies have shown that demanding activities such as supra-maximal cycling in humans (Gollnick et al., 1974) and jumping in the bushbaby (Gillespie et al., 1974) lead to a preferential recruitment of faster motor units. It is not, however,

known how widespread such strategies are across different types of locomotion or if there are any general patterns that govern the preferential recruitment of faster motor units. It is therefore apparent that our current understanding of muscle electrophysiology is incomplete.

Myoelectric signals result from the propagation of action potentials along the membranes of active muscle fibres. The resulting myoelectric signal is therefore an interference pattern, composed of action potentials from all the active motor units in the vicinity of the detecting electrode(s). The shape of the action potential is a function of the relative rates of membrane depolarisation to hyperpolarisation, a property that can vary between muscle fibre types (Adrian and Peachey, 1965; Albuquerque and Thesleff, 1968; Luff and Atwood, 1972; Stanfield, 1972). It should therefore be expected that different types of muscle fibres will generate motor unit action potentials with different shape and conduction velocity, indicating that a myoelectric signal will contain information about the types of motor unit active at any one time (Wakeling, 2005).

Methods to determine the amplitude and frequency components of myoelectric signals are well established (DeLuca, 1997). Amplitude of the signal can be distinguished using rectified signals or root mean squared values, while the signal frequency characteristics can be determined with the application of a Fourier transform. Such techniques have been invaluable in providing initial insights into changes in the frequency content of the myoelectric signal, and hence changes in motor unit recruitment, during different locomotor conditions. Fourier transform is, however, limited to analysing signals collected over a long time period (Kaiser, 1994; Mallat, 1998), meaning that motor unit recruitment during specific locomotor events, i.e. heel strike, cannot be distinguished using this technique. To overcome this, a myoelectric-specific wavelet approach has recently been described that is able to simultaneously resolve myoelectric signals into time and frequency space (von Tscharner, 2000). The wavelets are well defined in time and frequency, with the scaling adjusted to ensure a physiologically acceptable time resolution. This is an important consideration as the resolutions in time and frequency will inevitably be a compromise that satisfies the Heisenberg uncertainty principle, which states that the more precisely time resolution is defined the less precision is possible when defining the frequency component (Calude and Stay, 1995). The wavelet approach has been successfully applied in a number of reports of surface electromyography collected from humans during a range of tasks (Mundermann et al., 2006; von Tscharner, 2002; Von Tscharner and Goepfert, 2006; Wakeling et al., 2001a; Wakeling et al., 2001b), from *in situ* rodent muscle preparations (Wakeling and Syme, 2002) and from *in vivo* measurements of swimming fish and the slow walk and paw shake of the cat (Wakeling et al., 2002). These studies have shown that distinct high and low frequency components of the myoelectric signal can, respectively, be associated with activity in fast and slow motor units (Wakeling et al., 2002; Wakeling and Syme, 2002). Mammalian skeletal muscle is, however, composed of a range of different fibre types (Schiaffino and Reggiani, 1994), which show a continuum of shortening velocities (Bottinelli et al., 1994; Bottinelli et al., 1991) that will generate a range of myoelectric frequencies during any given activation. One of the current challenges is, therefore, to identify and quantify these variations, which are likely to be subtle, and use them to provide further insight into the electrophysiology of active muscle.

Principal component analysis is a powerful technique that can identify changes in spectral properties (Ramsay and Silverman, 1997) and has been successfully used to identify recruitment of fast and slow motor units in human leg muscles during cycling (von Tscharner, 2002; Wakeling et al., 2006). It provides a quantitative assessment of the change in the myoelectric spectral properties. Based on similar principles, a method of reconstructing the original myoelectric spectrum based on the linear superposition of two generating spectra that were associated with groups of fast and slow muscle fibres has recently been described (Von Tscharner and Goepfert, 2006). This enabled the interplay between groups of fast and slow muscle fibres to be estimated in the tibialis anterior and medial gastrocnemius muscles during running. Such techniques are in their infancy in terms of their application to the analysis of myoelectric signals. These initial reports, however, show that they are likely to form a powerful tool to enable more detailed analysis of recruitment patterns of different motor units within a muscle.

The soleus, plantaris and medial gastrocnemius muscles in the rat (*Rattus norvegicus*) act as plantar flexors around the ankle joint, with the plantaris and gastrocnemius also acting to flex the knee joint. The soleus is almost entirely composed of slow type I fibres (Table 1), and has been reported as having a maximum shortening velocity (V_{max}) of between 76.7±4.6 mm s^{-1} at 30°C (Caiozzo et al., 1992) and 80.0±4.8 mm s^{-1} at 30°C (Swoap et al., 1997). In contrast the plantaris is predominantly composed of type II fibres (Table 1), with the majority of these being classified as type IIA. V_{max} values between 149.6±3.7 mm s^{-1} at 30°C (Swoap et al., 1997) and 228.9±18.1 mm s^{-1} at 30°C (Caiozzo et al., 1992) have been reported. The medial gastrocnemius muscle contains distinct regions of slow, fast and mixed fibre types (Armstrong and Phelps, 1984). Fibres in the mixed region are predominantly type II, with the majority classified as type IIB (Table 1). V_{max} values have been reported for proximal (210±31 mm s^{-1}) and distal (262±20 mm s^{-1}) regions of the medial gastrocnemius muscle at 36°C (De Ruiter et al., 1995). The proximal region related to an area of red, slow oxidative fibres surrounded by a layer of faster white fibres, while the distal region was composed predominantly of fast white fibres (De Ruiter et al., 1995). The morphological differences between the soleus, plantaris and medial gastrocnemius muscles make them an ideal model with which to determine whether differences exist in motor unit recruitment patterns between muscles. In addition to this the value of wavelet analysis in determining patterns of motor unit recruitment both within and between muscles can also be assessed.

Table 1. *Reported populations of fibre types in the three ankle extensor muscles of the rat with maximum unloaded shortening velocity values*

Study information			Fibre type			
Muscle	Authors	Staining technique	Type I	Type IIA	Type IID/X	Type IIB
Soleus	(Norenberg and Fitts, 2004)	Myosin ATPase	89.4±3.1	10.6±3.1	–	–
	(Caiozzo et al., 1992)	SDS-PAGE	91.9±5.3	8.9±5.3	–	–
	(Armstrong and Phelps, 1984)	Myosin ATPase	87±4	13±4	–	–
	(Delp and Duan, 1996)	Myosin ATPase	84±6	7±0	9±6	0
Plantaris	(Caiozzo et al., 1992)	SDS-PAGE	5.1±0.6	63.4±4.1	–	31.5±3.8
	(Armstrong and Phelps, 1984)	Myosin ATPase	9±1	50±3	–	41±3
	(Delp and Duan, 1996)	Myosin ATPase	6±2	14±2	33±2	47±2
Medial gastrocnemius*	(Armstrong and Phelps, 1984)	Myosin ATPase	7±1	28±5	–	65±5
	(Delp and Duan, 1996)	Myosin ATPase	3±2	6±1	34±7	57±8
Force–velocity relationship	(Bottinelli et al., 1991)	V_{max} 12°C	0.64±0.04	1.40±0.08	1.45±0.07	1.8±0.11
	(Botinelli et al., 1994)	V_o 12°C	1.05±0.37	2.33±0.29	3.07±0.70	3.69±1.01

V_{max}, maximum unloaded shortening velocity ($L\ s^{-1}$); V_o, maximum unloaded shortening velocity calculated from slack test ($L\ s^{-1}$); SDS-PAGE, sodium dodecyl sulfate-polyacrylamide gel electrophoresis;

*Reports from the mixed region of medial gastrocnemius (defined by Armstrong and Phelps, 1984).

To date, the application of wavelet analysis to myoelectric signals collected *in vivo*, using fine-wire electrodes, has only been reported once (Wakeling et al., 2002). Principal component analysis has never been applied to data collected using fine-wire electrodes or to species other than man. These techniques, however, provide the tools with which a greater understanding of motor unit recruitment can be achieved. There is a growing body of evidence that suggests the predictions of the size principle, proposed by Henneman et al. (Henneman et al., 1965a; Henneman et al., 1965b), do not always hold true. In this paper we therefore aim to apply wavelet and principal component analysis techniques to determine whether the size principle holds true in the running rat, by studying three muscles with distinct fibre type populations. As the running stride can be considered as a series of events (e.g. foot on and initial limb loading, stance phase, foot off and swing phase) it might be expected that the motor unit recruitment patterns within the active muscles will vary to facilitate the changes in limb load, joint angle and force production required through out the stride. Indeed, it has previously been suggested that motor units may form specific task groups, which are selectively recruited within a stride (Loeb, 1985; Von Tscharner and Goepfert, 2006; Wakeling, 2004; Wakeling et al., 2001a). We therefore expect to see the myoelectric frequency content within each muscle vary across the time course of a stride, reflecting the different motor units being used for different locomotor tasks. Due to the distinct populations of fibre types within the three muscles studied it is also expected that signals from the soleus muscle will have a significantly lower frequency content than signals from the plantaris and medial gastrocnemius muscles. To this end we report the first analysis of *in vivo* myoelectric signals, collected from the three ankle extensor muscles of the rat, during treadmill locomotion using wavelet techniques. In addition, we provide a comparison of techniques that may be applied after wavelet analysis.

Materials and methods

Subjects

Myoelectric signals were collected from the soleus, plantaris and medial gastrocnemius muscles of the right hind limb of 11 female Sprague Dawley rats (approx. age 5–6 months), mean mass 245.75±22.92 g (± s.d.). The rats were grouped in pairs, housed in cages and maintained on standard rat feed [RM1 (E), Special Diet Services, Witham, Essex, UK]. The room was maintained at a temperature of approximately 20°C, with a 12 h:12 h light:dark cycle. Prior to the surgical procedures, animals were trained to run on a custom made, motorised treadmill at a range of speeds and inclines. Each rat was trained over a period of 5 weeks, ensuring that they were able to maintain a steady position on the treadmill belt for each speed/incline condition of interest. Due to the synchronous collection of sonomicrometry data and the small size of the muscles investigated, it was not possible to collect myoelectric data from each muscle in every subject. Table 2 lists the subjects from which data are presented. As muscle fibre length can significantly affect myoelectric frequency content (Doud and Walsh, 1995), it was important that changes in strain be considered in the analysis of these data so that significant differences in frequency content could be related to changes in motor unit recruitment rather than changes in fibre length. Strain measures from the sonomicrometry data are therefore included as a covariate in the statistical analysis of the myoelectric data, but do not form any other part of the work reported here. All procedures were performed in accordance with current UK Home Office regulations.

Surgical procedures

Rats were anaesthetised using halothane gas (4% induction; 1.75–2% maintenance), following a subcutaneous injection of atropine (0.01 mg kg^{-1}). The right hind limb and an area of the back in the region of the shoulder blades were shaved and scrubbed with 4% chlorhexidine gluconate solution (E-Z

Table 2. *Subjects from which each data set was collected*

Subject number	Muscle		
	Soleus	Plantaris	Medial gastrocnemius
1	X	X	
2	X		X
3	X		X
4	X		
5			X
6	X		
7	X	X	
8	X		
9		X	
10		X	X
11		X	X

Data sets (X) were collected from rats at 0° incline, while running at 40 cm s^{-1}.

Scrub, Becton, Dickinson and Co., Franklin Lakes, NJ, USA) and painted with a povidone–iodine solution. An ocular lubricant (Lacri-Lube®, Allergan Ltd, Marlow, UK) was applied to each eye. A small incision, approximately 30 mm long, was made along the lateral aspect of the limb over the fascia of the biceps femoris and approximately parallel with the tibia. A second skin incision was made caudal to the scapulae and a subcutaneous tunnel created between the two incisions. Wires from each of the transducers to be implanted were fed through the tunnelling device before its removal. After implantation of the electrodes, excess wire externalised at the site of the second incision, at the shoulder blades, was wound into a small coil and placed inside a cotton pouch.

Fine tip forceps were used to insert offset twist-hook bipolar silver-wire electrodes (0.1 mm diameter, California Fine Wire Inc., Grover Beach, USA), with tips bared of 0.5 mm of insulation into the muscles of interest (Loeb and Gans, 1986). The depth of the implantation was approximately 3 mm with approximately 2 mm separating the tips in each muscle. In the medial gastrocnemius electrodes were placed in the medio-caudal region of the muscle, which has been identified as containing a mixture of fibre types (Armstrong and Phelps, 1984). In the soleus and plantaris muscles electrodes were placed in the mid-belly of the muscle. The wires were secured to superficial fibres of the muscle using 5-0 prolene suture to prevent them being dislodged. Slack wire was fed under the skin in the area surrounding the hip to ensure the animal had the full range of motion of the hind limb, and was not restricted by the presence of the wires. The fascia and skin incision were sutured shut using 5-0 vicryl suture. To secure the pouch containing the externalised wires a small jacket was fashioned for each subject using elasticated bandage (Vetrap™, 3M United Kingdom PLC, Bracknell, UK). This protected the wound and the wires at the nape of the neck and enabled rats to be kept in their pairs during the recovery period. Post-operative analgesia (buprenorphine, 0.01 mg kg^{-1}, s.c.) was administered during the 48 h recovery period.

Data collection

All data were collected in an electrically shielded room. Two cameras (A602f, Basler, Ahrensburg, Germany), running off digital triggers and connected to the data collection computer using IEEE 1394 ports, were used to record the position of the right hind limb in the stride (100 frames s^{-1}), for each trial. Myoelectric signals (3200 Hz) were amplified (CP511 A.C. amplifier, Astro-Med, Inc., West Warwick, RI, USA), with a bandpass filter of 30–1000 Hz and collected through a 16-bit data acquisition card (PCI-6221, National Instruments Corp., Austin, TX, USA). Myoelectric and video data were collected for periods of 30 s of running, after being synchronously triggered *via* the data acquisition card. Custom written software (LabView 7.1, National Instruments Corp.) synchronised collection of myoelectric signal and video data streams.

Rats ran a three-block, randomised exercise programme incorporating a number of speed and incline combinations. For the purposes of this work the results from 0° incline at 40 cm s^{-1} are presented. On completion of the protocol, animals were euthanized with intraperitoneal pentobarbitone and the position of the electrodes verified through dissection.

Analysis of data

Wavelet transformation and filtering of the myoelectric signal

A filter bank of 20 non-linearly scaled wavelets, indexed by k (0–19 inclusive), were used to decompose the myoelectric signals into their intensities, i, as a function of time and frequency (given by wavelet domain k). For any time point the myoelectric intensity at wavelet domain k is therefore denoted as i_k. In the following description the myoelectric intensity spectrum at any given time point is described as a function of the centre frequencies of its component wavelet domain $i(f)$. Each wavelet domain was described by its frequency bandwidth, centre frequency (f_c) and time resolution using the methods described (von Tscharner, 2000).

Previous analysis of Fourier transform derived power spectra from the myoelectric signal from each muscle indicated that a quantity of low frequency noise was included in the signal. Each power spectrum was normalised to the power within the 400–600 Hz region. From the normalised power spectra, one subject was chosen to represent a template of a clean signal for each muscle (Fig. 1A). The template was defined as a smooth, bell-like curve, with minimal low frequency (<100 Hz) components. A cut-off frequency was defined as the frequency at which the difference between the template spectrum and the other spectra for that muscle was zero (Fig. 1B). Each muscle showed a different cut-off frequency, with a large amount of variation, contained in wavelet domains 3, 4 and 7 (soleus 55.21±24.29 Hz; plantaris 208.00±10.19 Hz; medial gastrocnemius 92.31±35.14 Hz; means ± s.d.). To assess the cut-off point that would be most suitable for all the muscles, a cumulative assessment of the proportion of the myoelectric intensity in each wavelet domain was conducted in the subjects previously used as template power spectra. The assessment showed that excluding the first four wavelet domains from

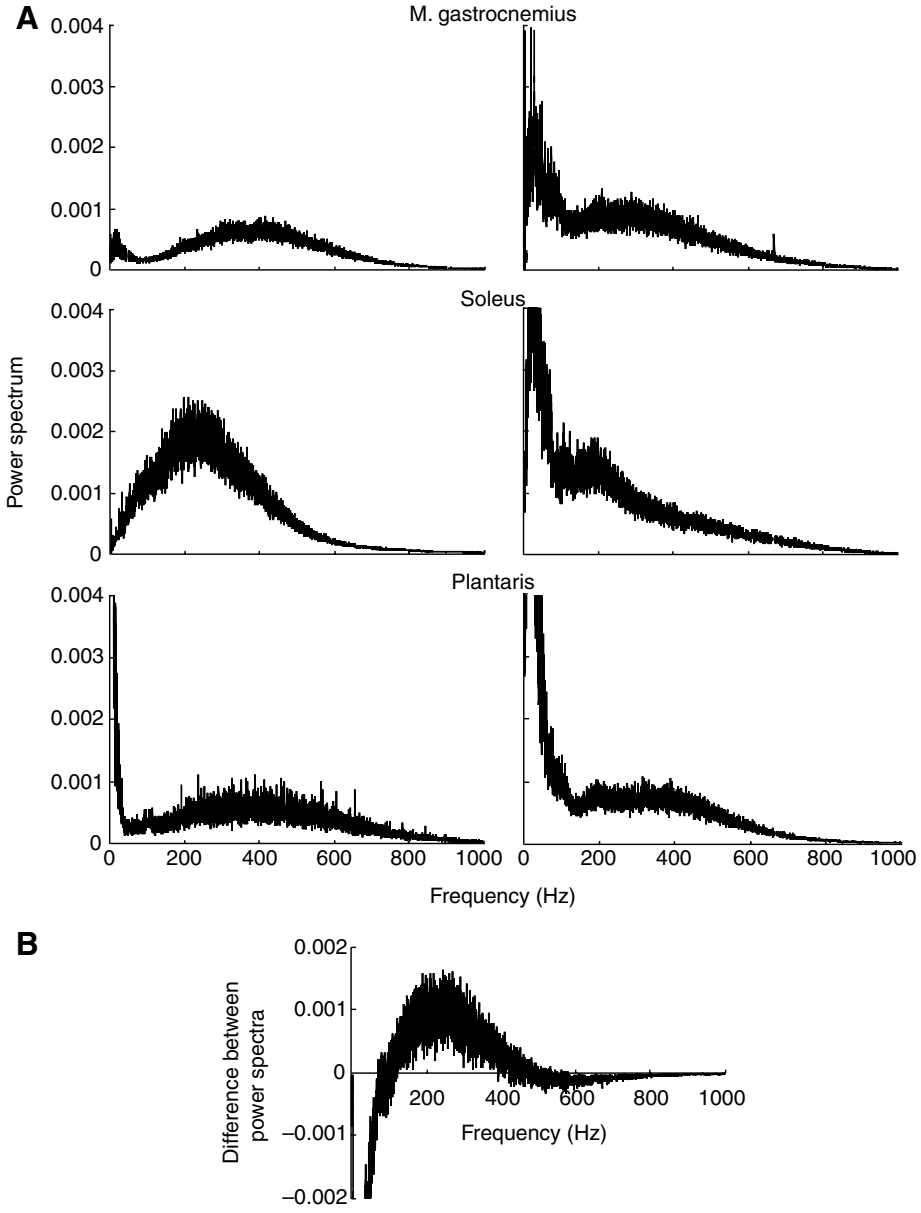

Fig. 1. (A) The three power spectra representing a clean signal (left panels), with examples of power spectra from subjects with a large low frequency component (right panels). (B) Example of a graph used to determine the transition between real signal and noise in the soleus muscle.

further analysis would mean that approximately 95% of the original myoelectric signal would be included in the analysis (soleus 94.39%; plantaris 92.71%; medial gastrocnemius 97.09%). Excluding the first five wavelet domains would ensure that approximately 90% of the signal would be included (soleus 89.42%; plantaris 90.55%; medial gastrocnemius 95.53%). The decision was therefore taken to exclude the first four wavelet domains from further study, therefore the analysis will consider the frequency band 69.92–1325.00 Hz (wavelets $4 \leqslant k \leqslant 19$). Although this cut-off frequency will not remove all low frequency noise in the myoelectric signals collected, particularly in the plantaris muscle, it will filter a large proportion of low-frequency noise. Further to this, slow motor units have been reported as having a mean frequency of 183.3±7.9 Hz (Wakeling and Syme, 2002), indicating that the cut-off frequencies selected here will ensure signals from these motor units are preserved. The cut-off point selected also corresponds well to the filtering used in previously reported fine-wire myoelectric studies; 100 Hz (Daley and Biewener, 2003; Gillis and Biewener, 2001; Gillis and Biewener, 2002); 150 Hz (Gabaldon et al., 2004).

Analysis of the wavelet transformed myoelectric signal

Data were initially analysed as complete strides, defined by consecutive foot on times taken from the foot of the right hind limb (1178 strides: 340 soleus strides; 364 plantaris strides; 477 medial gastrocnemius strides). Analyses were also conducted on each stride partitioned into 20 equal time-windows. The total intensity of the signal at a given time was given by summing the intensities over the selected k wavelets ($4 \leqslant k \leqslant 19$). This provides a measure of the power within the signal over time at well-defined intervals. In comparison with root mean square values, which are measures of amplitude, half the intensity obtained from wavelet analysis is comparable with the square of the root mean square value. The mean intensity spectrum was calculated as the mean intensity occurring at each of the wavelet domains and was calculated for each whole stride and the sectioned portions of each stride. To facilitate comparison between subjects the mean spectra were normalised to unit area of spectra calculated from running at 40 cm s^{-1} on a 10° incline. These data were collected during the same protocol, but are not included in any further analysis here. The instantaneous mean frequency (f_m) at each sample point was determined from:

$$f_m = \frac{\sum_k f_c(k) i_k}{\sum_k i_k}, \quad (1)$$

with the mean frequency calculated as the mean of f_m values taken from whole strides.

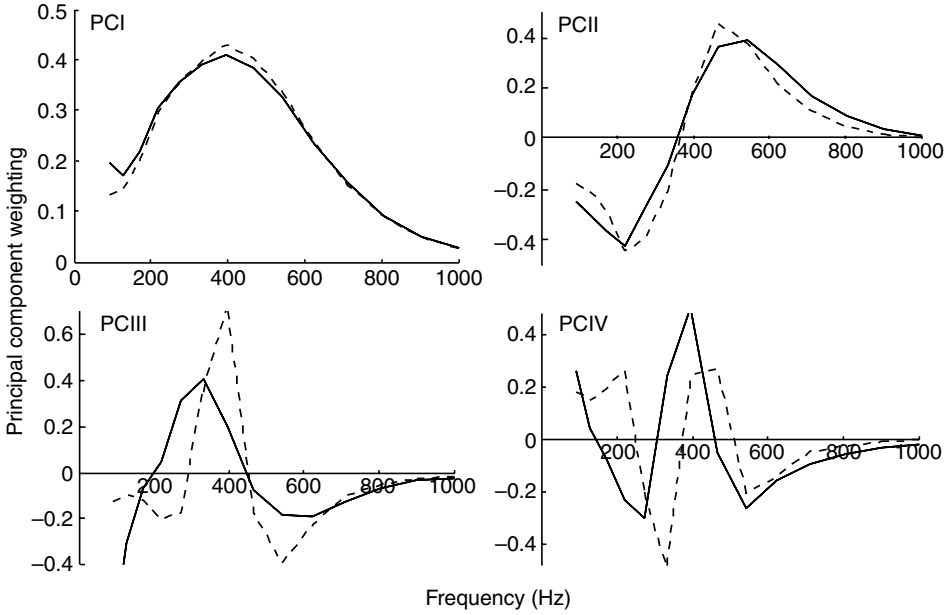

Fig. 2. The principal component weightings for the first four principal components (PCI–IV) from spectra from whole strides (solid lines, *N*=1178) and partitioned strides (broken lines, *N*=23 560).

Principal component analysis

Principal component analysis transforms a data set to a reduced number of dimensions that describe the major features in the data. In the present example it can be considered that the data set are described by 16 components, as each spectrum contains p=16 dimensions (wavelet domains). These were aligned into a $p\times N$ data matrix **A**, where N indicates the number of trials/spectra included in the analysis. The principal components were calculated from the total intensity data without prior subtraction of the mean; this ensured they would describe the whole signal and not just its variance (Wakeling and Rozitis, 2004). The covariance matrix **B** was calculated for data matrix **A**:

$$\mathbf{B} = \mathbf{A}^{\mathrm{T}} \cdot \mathbf{A} \cdot (1/N–1) \, . \qquad (2)$$

The principal components, defined in terms of eigenvector–eigenvalue pairs, were then calculated for matrix **B**. Each principal component is made up of a set of orthogonal eigenvectors (ξ), with the eigenvalues representing the variability that can be explained by the corresponding principal component (Ramsay and Silverman, 1997). The principal components were ranked in descending order of the magnitude of the amount of the original spectra they were able to explain. The first few principal components were able to explain a large proportion of the original spectra (PCI 88.95%; PCII 5.03%; PCIII 1.48%; PCIV 0.99%; Fig. 2). It was therefore possible to express the spectra in fewer terms than the original suite of wavelets used (Wakeling and Rozitis, 2004). The principal components were represented in two ways:

(1) The principal component weighting, given by its eigenvector ξ, displayed graphically as a function of the central frequency of the corresponding wavelet (Wakeling and Rozitis, 2004);

(2) The principal component loading score given by the eigenvalue calculated from $\xi^{\mathrm{T}}\mathbf{A}$. These are scalar quantities that describe the amount of each ξ present in each myoelectric signal. Once the principal component weightings have been identified each spectrum can be visualised by its principal component loading score (Ramsay and Silverman, 1997; Wakeling and Rozitis, 2004).

For the principal component weightings identified in this analysis, the angle formed between the PCI and PCII loading scores (θ) provides a quantitative measure of the contribution of high and low frequency content in the myoelectric signal. A small θ, defined by a positive contribution of the PCII loading scores, indicates a proportionally higher amount of high frequency content. A larger θ, defined by a negative PCII contribution, indicates a higher contribution of low frequency content. PCI loading scores have been shown to correlate with total myoelectric intensity (Wakeling, 2004), and hence are a good indicator of myoelectric activity. Differences in PCII loading scores when PCI loading scores are found to be equal therefore indicate differences in the motor units recruited (Wakeling, 2004). Principal components were calculated for each complete stride and also for each of the sectioned portions of the stride, enabling changes in the relative contribution of PCI and PCII to be defined for different time points within each stride.

Optimising signal analysis to high and low frequency bands

The first principal component can be related to the intensity of the myoelectric signal and the relative PCI and PCII loading scores describe the frequency content of the signal (Wakeling and Rozitis, 2004). Myoelectric intensity spectra [$i(f)$] can therefore be reconstructed from a linear combination of the principal component weightings:

$$i(f) \approx q(\xi_{\mathrm{PCI}} + a\xi_{\mathrm{PCII}}) \, , \qquad (3)$$

where q scales the intensity to normalised levels and a represents the relative amount of PCII to PCI loading scores. As intensity spectra represent the power within the myoelectric signal they must have non-negative intensities at all frequencies. The extreme positive and negative values for a, a_{f} and a_{s}, respectively, that satisfy this condition form two solutions to Eqn 3 (Fig. 3). For each of these extremes a wavelet was constructed to describe the spectra using least

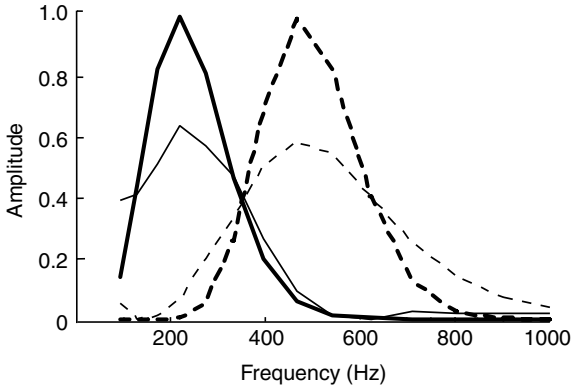

Fig. 3. Reconstructed spectra [$i(f)$] calculated for a_s (solid thin line) and a_f (broken thin line) in Eqn 3, overlaid with optimised wavelets ψ_s (solid bold line) and ψ_f (broken bold line).

squares minimisation of a wavelet function $\psi(f)$ to the intensity spectrum $i(f)$ where:

$$\psi(f) = \left(\frac{f}{f_c}\right)^{f_c \cdot \text{scale}} e^{\left(\frac{-f}{f_c}+1\right)^{f_c \cdot \text{scale}}}, \quad (4)$$

and 'scale' is a scaling factor defining the width/shape of the function (von Tscharner, 2000). The two defined wavelets were termed $\psi_f(f)$ and $\psi_s(f)$ for high and low frequency domains, respectively (Table 3; Fig. 3). The frequency bandwidth was defined as the frequencies at which the magnitude of the wavelet was $1/e$ of its maximum value. The time resolution was calculated as the time at which the intensity of the wavelet was $1/e$ of its maximum (von Tscharner, 2000). The resulting models were normalised to unit area of $i(f)$ calculated from a_f and a_s, respectively. Each measured myoelectric intensity spectrum, $i(f)$, was then represented by the linear combination of the optimised wavelets ψ_f and ψ_s and their loading scores C_f and C_s, using non-negative factorisation with:

$$i(f) \approx C_f\psi_f(f) + C_s\psi_s(f) . \quad (5)$$

C_f and C_s were calculated for each time point to give the time-varying $C_f(t)$ and $C_s(t)$.

Statistical analysis

Two-way ANOVA were conducted to determine differences in the mean frequency, principal component loading scores and θ from each stride between the muscles. In all instances muscle was defined as a fixed factor and individual as a random factor. ANCOVA was used to determine differences in the mean θ within each muscle from each time window, with mean muscle fascicle strain for the corresponding time window used as the covariate. ANCOVA was also used to determine the effect of subject, time window and PCI on PCII within each muscle, with PCI defined as the covariate. When significant differences were identified Bonferroni *post-hoc* test was used to identify the location of the significant differences. In all instances results were considered to be significantly different when $P<0.05$. The association between PCI and mean myoelectric intensity was determined using Pearson product–moment correlation. The goodness-of-fit of the optimised wavelets was calculated as the coefficient of determination (r^2) between the total myoelectric intensity from the stride and the intensity calculated for $C_f(t)$ and $C_s(t)$ combined and as individual factors. The correlation between $C_f(t)$ and $C_s(t)$ was also compared in each muscle. MANOVA was used to determine if r^2 values from the fit of ψ_s and ψ_f to total intensity were significantly different between muscles. In addition to this MANOVA was used to determine if the correlation between $C_f(t)$ and $C_s(t)$ differed significantly to the relationship between total intensity and the combined value of $C_f(t)$ and $C_s(t)$. All results are reported as mean ± standard error of sample mean (s.e.m.).

Table 3. *Parameters of optimised wavelets ψ_s and ψ_f*

Wavelet	Centre frequency, f_c (Hz)	Frequency bandwidth (Hz)	Time resolution (ms)	Scale
ψ_s	206.28	151.11	1.88	0.033
ψ_f	458.00	225.05	3.13	0.047

Results

Differences in myoelectric frequency content between muscles

Intensity spectra from each of the muscles are shown in Fig. 4. The spectrum from the soleus muscle had a relatively larger proportion of low frequency signal, while the plantaris and medial gastrocnemius muscles had similar traces, particularly at frequencies above 400 Hz. Significant differences in mean frequency were identified (Table 4, $P=0.049$), with the differences occurring between each of the muscles ($P<0.001$ in all cases; soleus 370.11±1.71 Hz, $N=340$; plantaris 386.94±2.32 Hz, $N=364$; medial gastrocnemius 422.23±2.02 Hz, $N=477$).

When data were assessed from whole strides the first two principal components explained 93.98% of the myoelectric signal, with the third and fourth components explaining a further 2.47% (Fig. 2). The first principal component had a positive weighting for all frequencies, with the peak occurring at wavelet domain 10 (f_c=395.44 Hz). The shape of the component was similar to the mean intensity spectra for the data (Fig. 4), with a very strong correlation occurring in each muscle between PCI and the mean intensity (for all muscles $r^2=0.99$). The second principal component had both negative and positive weightings. Peaks occurred at wavelet domains 7 and 12, respectively (f_c=218.07 and 542.06 Hz; Fig. 2), with the transition between negative and positive portions occurring between wavelet domains 9 and 10 (f_c=330.62 and 395.44 Hz). The medial gastrocnemius muscles had a positive PCII loading score, while the soleus had a negative loading score (Fig. 5). The third principal component also had both positive and negative features. In this instance the component was negative from wavelet domains 4–6 (f_c=92.36 Hz and 170.39 Hz),

Table 4. *Details of results of the two-way ANOVAs used to assess differences between muscles*

	Factor								
	Muscle			Subject			Muscle×subject		
Dependent variable	*F*	d.f.	*P*	*F*	d.f.	*P*	*F*	d.f.	*P*
Mean frequency	7.00	2	0.049	2.69	10	0.176	105.40	4	<0.001
θ	6.12	2	0.060	2.37	10	0.211	99.11	4	<0.001
PCI loading score	0.60	2	0.591	0.89	10	0.601	163.63	4	<0.001
PCII loading score	0.62	2	0.187	1.03	10	0.534	189.63	4	<0.001
PCIII loading score	3.49	2	0.129	3.71	10	0.109	11.79	4	<0.001

Muscle was defined as a fixed factor, subject as a random factor; θ = angle between PCI and PCII loading scores.
Muscle × subject = interaction between the two factors; d.f., degrees of freedom.

positive from wavelet domains 7–10 (f_c=218.07 Hz and 395.44 Hz) and negative again from wavelet domain 11 onwards (f_c=465.92 Hz). ANCOVA showed there was no significant relationship between PCI and PCII loading scores (P=1.00), while ANOVA showed that θ did not differ significantly between each of the muscles (P=0.06; Table 4, Fig. 6).

Interplay between low- and high-frequency bands

Each muscle showed one complete burst of activity during a stride, with the relative duration differing between the muscles (soleus 36.7%; plantaris 67.6%; medial gastrocnemius 31.4%) (Fig. 7A). Defining the intensity of the signal with $C_s(t)$ and $C_f(t)$, revealed differences in the interplay between high and low frequency components of the myoelectric signal within a stride (Fig. 7A). In the soleus and medial gastrocnemius $C_s(t)$ and $C_f(t)$ were, respectively, the dominant feature of the signal through the whole stride. In the plantaris muscle, $C_s(t)$ was initially greater between approximately 60–90% stride (approx. 104 ms), while $C_f(t)$ was greater during the early (0–40% stride, approx. 139 ms) and late (90–100% stride, approx. 35 ms) stages of the stride. The goodness-of-fit of the reconstructed signal from Eqn 5 to the total intensity was high in each of the muscles (soleus, r^2=0.99±0.005; plantaris, r^2=0.98±0.008; medial gastrocnemius, r^2=0.99±0.004). The r^2 value for the fit of $C_f(t)$ was significantly greater in the medial gastrocnemius muscle compared to the soleus and plantaris muscles (P<0.001). In contrast the r^2 value for $C_s(t)$ was significantly greater in the soleus muscle compared to plantaris and medial gastrocnemius (P<0.001). Assessment of the correlation

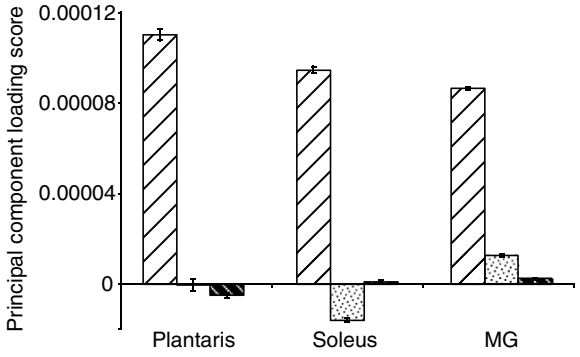

Fig. 5. Principal component loading scores for PCI (diagonal hatch), PCII (speckled) and PCIII (dark hatch) for each muscle, calculated from data taken from whole strides. Values are means ± s.e.m.

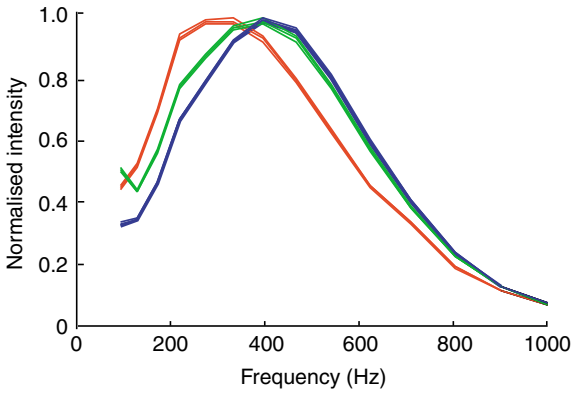

Fig. 4. Mean myoelectric intensity from whole strides for soleus (red, N=344), plantaris (green, N=364) and medial gastrocnemius (blue, N=477), normalised to unit area. Traces show means ± s.e.m.

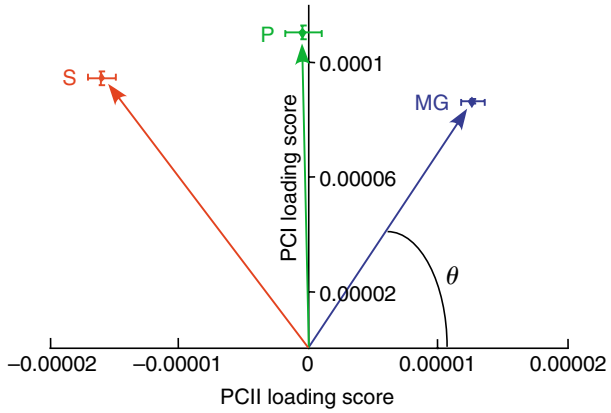

Fig. 6. PCI and PCII loading scores for soleus (S, N=340), plantaris (P, N=364) and medial gastrocnemius (MG, N=477). Values are calculated from the data taken from whole strides. θ was calculated as the angle formed between PCI–PCII loading score vector and PCII loading score axis. Values are means ± s.e.m.

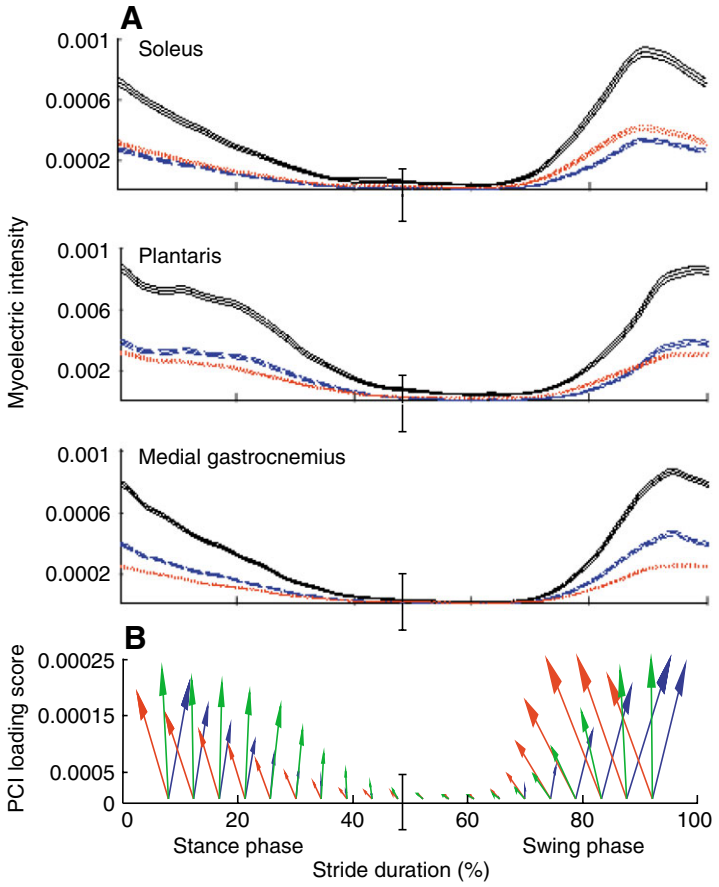

Fig. 7. (A) Mean myoelectric intensity (black, solid line) for soleus (N=340), plantaris (N=364) and medial gastrocnemius (N=477) muscles, showing interplay between $C_s(t)$ (red dotted line) and $C_f(t)$ (blue broken line). All values are means ± s.e.m. (B) Vector plot of PCI and PCII loading scores in the soleus (red, N=340), plantaris (green, N=364) and medial gastrocnemius (blue, N=477); each arrow represents a different time point during the stride. The vertical line in each diagram denotes the transition from stance to swing phase.

between $C_s(t)$ and $C_f(t)$ revealed much lower values for r^2 within each of the muscles (soleus, r^2=0.61±0.093; plantaris, r^2=0.54±0.091; medial gastrocnemius, r^2=0.61±0.084). These were significantly less than the fit found between total intensity and both $C_s(t)$ and $C_f(t)$ (P<0.001 in each case), and between total intensity and combined values of $C_s(t)$ and $C_f(t)$ (P<0.001).

Changes in myoelectric frequency content during a stride

When the stride was partitioned into time windows the first few principal components explained less of the myoelectric signal than when the stride had been analysed as a whole (PCI 72.13%; PCII 7.66%; PCIII 4.17%; PCIV 3.49%). The trends seen in the principal component weightings were, however, very similar to those found from the analysis of the stride as a whole (Fig. 2). When comparing θ, distinct differences were apparent between the muscles and between portions of the stride. Comparison of θ within each muscle, with strain included as a covariate, showed significant differences between

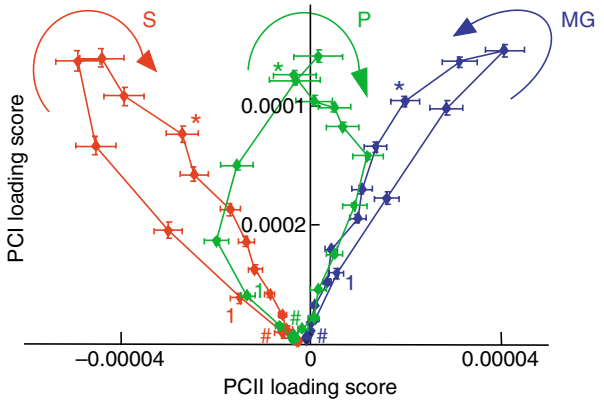

Fig. 8. PCI and PCII loading scores at partitioned time points during a stride for the soleus (S, N=6880), plantaris (N=7280) and medial gastrocnemius (MG, N=9540) muscles. Values are means ± s.e.m. Asterisks indicate foot on, 0% stride duration; hash marks indicate foot off. Note that in each muscle, activity begins during the swing phase, therefore the direction of each loop is indicated by the arrows; 1 indicates the beginning of myoelectric activity.

many of the time windows (P<0.001 in all cases; Fig. 8). The soleus muscle always had a negative PCII loading score with greater values, and hence larger θ, occurring during the later time windows within the stride. The medial gastrocnemius always had a positive PCII loading score, although in contrast to the soleus and plantaris muscles larger θ values were found during the initial stages of the stride. The most variation in PCII loading scores and θ was seen in the plantaris muscle. The PCII loading score was positive during the initial part of the stride corresponding to small θ values, and negative during the later stages of the stride, corresponding to larger θ values. Changes in the PCI loading score also varied within the stride. Each muscle had a similar maximum PCI loading score (soleus, $2.59\pm0.00\times10^{-3}$; plantaris, $2.57\pm0.00\times10^{-3}$; medial gastrocnemius, $2.55\pm0.00\times10^{-3}$); however, the change in PCI over time differed between the muscles. The soleus and medial gastrocnemius showed similar PCI loading scores at each time point. The PCI loading score in the plantaris muscle was consistently higher during the first 45% of the stride and lower between 75–90% of stride duration. This trend is also apparent in the plot of θ as a function of time (Fig. 7B).

Discussion

The relationship between myoelectric signal characteristics and fibre type

The methods presented in this report offer a more detailed level of analysis of myoelectric data than has previously been described for the rat. The three muscles studied represent a range of fibre type combinations, providing an opportunity to distinguish differences in the myoelectric signal from a predominantly slow muscle fibre population (soleus), a predominantly fast muscle fibre population (medial gastrocnemius) and a mixed population of fibre types

(plantaris) (Table 1). The significant differences in the properties of the myoelectric signals between the muscles during a stride indicate that differences in fibre type populations can be identified in the myoelectric signal using the techniques described. A significant negative correlation between mean myoelectric frequency and proportion of type I fibres has been reported previously (Gerdle et al., 1988). In agreement with this, the results of the present study show that the soleus muscle had the lowest mean frequency (370.11±1.71 Hz), while the faster medial gastrocnemius had the highest mean frequency (422.23±2.02 Hz). Slow and fast motor units in the rat have, however, been reported as having a much lower mean frequency of 183.30±7.90 and 369.30±10.80 Hz, respectively (Wakeling and Syme, 2002). This difference is likely to relate to differences in methodologies used, in particular the use of bipolar *versus* monopolar electrodes. In addition to this, measures by Wakeling and Syme (Wakeling and Syme, 2002) were taken using an *in situ* nerve blocking technique that ensured only the slowest or fastest motor units were active. The myoelectric signals presented here are from whole muscle and therefore represent signals from a larger range of motor units, and will also reflect the fact that a range of maximum shortening velocities exist within fibres with the same myosin heavy chain isoforms (Bottinelli et al., 1994; Bottinelli et al., 1991).

Traditionally power spectra, derived from Fourier transforms, have been used to identify changes in the frequency content of the myoelectric signal, as they enable the calculation of mean and/or median frequency values. Such values provide an initial assessment of the frequency content of the signal and, in the past, have been useful indicators of muscle fatigue (Brody et al., 1991; Petrofsky, 1979) and for the identification of when different types of motor unit are active (Elert et al., 1992; Gerdle et al., 1988). In this study we applied principal component analysis to identify and quantify differences in myoelectric signal intensity and frequency content between different populations of fibre types. When the data set was partitioned into complete strides the first three principal components were able to describe over 95% of the signal, matching previous reports (von Tscharner, 2002; Wakeling and Rozitis, 2004; Wakeling et al., 2006). The results of this study and previous work (Wakeling and Rozitis, 2004) show that PCI closely matches the mean intensity spectrum of the myoelectric signal and therefore represents the intensity of the signal, while PCII represents the relative contribution of each frequency component to the signal. Each measured myoelectric intensity spectrum can be reconstructed by the linear combination of the PC weightings and the PC loading scores. The relative contribution of the PCI and PCII loading scores would lead to a skewing of the myoelectric spectra to lower or higher components (Eqn 3). This is demonstrated by the frequency content of the soleus and medial gastrocnemius muscle, which have, respectively, the lowest and highest mean frequency values and PCII loading scores (Fig. 5). The third principal component had two negative phases with a positive phase occurring in the mid-range of frequencies (200–400 Hz). The combination of PCIII with PCI would therefore lead to a broadening or narrowing of the reconstructed spectrum. Data from the whole stride showed that the plantaris muscle had a large negative PCIII loading score, which would lead the intensity spectrum to be narrower, and become centred on the mid-range frequencies rather than skewed to the low or high frequencies. Although not significantly different, the PCIII loading score in soleus and medial gastrocnemius was smaller than in the plantaris and in comparison to their respective PCII loading scores (Fig. 5), indicating that in these muscles PCI and PCII are the main contributors to the frequency spectrum, while in the plantaris muscle PCI and PCIII can be considered the more dominant factors. As both PCII and PCIII have close to zero integral they will have little effect on the intensity of the reconstructed spectra; however, the results indicate that they both play a role in determining the shape of the spectra.

The frequency content of the signal was further quantified by θ, which was defined by the direction of the vector of the PCI–PCII loading score (Fig. 6) (Wakeling and Rozitis, 2004; Wakeling et al., 2006). Statistical analysis showed that there was no significant difference in θ between muscles when the stride was assessed as a whole (Table 4). When data were partitioned into equal time windows the value of this variable for quantitatively determining differences in the frequency content of the myoelectric signal was shown (Fig. 8) and indicates the value of subjecting myoelectric signals to more sensitive methods of analysis.

Task-specific recruitment of motor units

The principle aim of this work was to determine whether the size principle holds true in the running rat by identifying changes in motor unit recruitment through the time course of a stride. Partitioning the data into equal time windows revealed the variability that occurs through a stride, which was demonstrated by the fact that less of the myoelectric signal was explained by PCI-III (83.96 *versus* 95.46%). The main features of these major principal components are, however, preserved (Fig. 2), indicating that the same components are identified whether the data are assessed as complete or partitioned strides. The fact that the first three components represent a smaller proportion of the spectra indicates that the properties of myoelectric signals vary over the course of a stride, and that investigation of such changes is warranted. In agreement with the prediction that myoelectric frequency content would vary across the time course of a stride, the assessment of θ calculated from the time windows of the stride highlighted striking differences both within and between the muscles. The PCI–PCII loading scores in the PCI–PCII loading score plane showed a marked hysteresis, with the largest loop representing the plantaris muscle (Fig. 8). As PCI represents the myoelectric intensity and PCII represents the relative contribution of the frequency components, such hysteresis must represent changes in the motor units recruited, particularly when the same PCI loading score occurs with different PCII values (Wakeling, 2004). The results presented here therefore clearly show that a specific myoelectric intensity value is not the result of a single

motor unit recruitment pattern, as would be predicted by the size principle. Indeed it is apparent in all the muscles studied that much more variation in recruitment patterns exists than would previously have been expected.

The direction of the hysteresis loops is determined with the myoelectric activity being considered as one complete burst (i.e. from mid-swing to mid-stance) (Fig. 8). Differences between the muscles are apparent, with soleus and plantaris looping clockwise, while medial gastrocnemius looped anti-clockwise. This indicates that for rats running on a level treadmill at $40\,cm\,s^{-1}$ the soleus and plantaris muscles demonstrate sequential recruitment of faster motor units. The pattern of recruitment is, however, reversed in the medial gastrocnemius muscle, with faster motor units recruited prior to slower ones, further contravening the predictions made by the size principle. Such a recruitment pattern does, however, appear to suggest a mechanical basis for motor unit recruitment. Muscle fascicle contractile properties are related to V_{max}. Maximum mechanical power generation has been shown to occur at 0.25–0.36 V_{max} (Swoap et al., 1997), while maximum mechanical efficiency occurs between 0.15–0.29 V_{max} (He et al., 2000). This indicates that to generate mechanical power at a high efficiency it would be preferable to recruit faster motor units for faster contractions (Rome et al., 1988). In the future it would be of interest to determine whether fibre type recruitment is matched to the muscle shortening velocities during different movement tasks in different muscles. Such an association has already been identified in the medial gastrocnemius of humans during cycling (Wakeling et al., 2006), and it would therefore be of interest to determine how widespread such a phenomenon is.

Several factors have been shown to affect the frequency content of the myoelectric signal, and so must be considered when interpretations are made. For example, longer fibre lengths are known to result in lower frequency content (Doud and Walsh, 1995). The inclusion of strain as a covariate in the statistical analysis, however, ensures that the differences identified here are the result of changes in motor unit recruitment and not changes in fibre length. Secondly, fatigue and muscle temperature must also be considered as potential influences (Petrofsky, 1979; Stalberg, 1966); however, the randomised, three block exercise protocol that was used to collect data will remove any bias introduced by these factors (Wakeling et al., 2006) and the time course within each stride is too short for this to have been a significant factor. It has been previously suggested that motor units may form task groups, which are selectively recruited for different kinematic conditions within a stride (Loeb, 1985; Von Tscharner and Goepfert, 2006; Wakeling, 2004; Wakeling et al., 2001a). We have been able to provide evidence to support this suggestion and have identified that different recruitment patterns also occur between different muscles. A number of examples where the size principle does not hold true have previously been reported for cats (Hoffer et al., 1981; Grimby and Hannerz, 1977; Kanda et al., 1977), jumping in the bushbaby (Gillespie et al., 1974) and humans (Gillespie et al., 1974; Grimby and Hannerz, 1977; Hoffer et al., 1981; Kanda et al., 1977; Nardone et al., 1989; Wakeling, 2004; Wakeling et al., 2006). Our results are the first example to be found in the rat and highlight an area of research where our current understanding is limited. The opportunity therefore exists to use the techniques described here to identify factors that govern the preferential recruitment of faster motor units in situations where the size principle does not hold true and to increase our understanding of motor control, thus making a significant contribution to fields such as neuromuscular physiology.

Visualising interplay between myoelectric intensities in low- and high-frequency bands

Defining optimised wavelets ψ_s and ψ_f enabled the changes in the high and low frequency component of the myoelectric signal to be visualised over time. The goodness-of-fit of $C_f(t)$ and $C_s(t)$ varied between the muscles and again highlighted the differences in the frequency content of the signals over time and differences between the three muscles studied. The significantly better fit between the total intensity from the soleus muscle and $C_s(t)$ indicates that ψ_s is able to describe more of the myoelectric signal from a population of predominantly slow muscle fibres. ψ_f is shown to describe more of the myoelectric signal from a population predominantly composed of the fastest muscle fibres, as there was a significantly better fit between the total intensity from the medial gastrocnemius muscle and $C_f(t)$.

High/low frequency band ratios have previously been used to identify changes in myoelectric signals that occur due to fatigue. In general the bands have been arbitrarily defined, with the low and high bands described as occurring between 15–45 and 45–95 Hz (Allison and Fujiwara, 2002), 20–40 and 130–238 Hz (Bai et al., 1984; Esau et al., 1983) and 20–46.7 and 150–350 Hz (Gallagher et al., 1985). These reports found good correlation between median frequency values and the high/low band frequency ratios and have been used to determine the proportion of the total integrated EMG that each frequency band contributes to (Allison and Fujiwara, 2002). More recently attempts have been made to relate high and low frequency bands specifically to fast and slow motor unit activity. Mundermann et al. (Mundermann et al., 2006) defined a low frequency band between 25–82 Hz (wavelet domains $2 \leqslant k \leqslant 3$) and a high frequency band between 142–300 Hz (wavelet domains $6 \leqslant k \leqslant 8$), for the analysis of myoelectric signals collected using surface electrodes. These bands were defined after wavelet transformation of the myoelectric signal and were chosen based on previous work (Wakeling et al., 2001a); however, they were not optimised to the myoelectric intensity spectrum. In a similar technique to that presented here, Von Tscharner and Goepfert (Von Tscharner and Goepfert, 2006) also used wavelet analysis transformation before focussing on defining two spectra, based on Eqn 4, with which the original spectra could be reconstructed. The methods presented here, however, offer a faster computational option as ψ_s and ψ_f are optimised to the spectra once, while in the methods described by Von Tscharner and Goepfert (Von

Tscharner and Goepfert, 2006) optimisation occurs for each individual spectrum. Determining frequency bands using optimisation techniques leads to an overlap in the defined bands (Fig. 3), which does not occur when bands are arbitrarily chosen. The overlap is likely to represent the continuum that exists in the shortening velocities between and within the different fibre types (Bottinelli et al., 1994; Bottinelli et al., 1991); however, it does mean that the two bands are not totally independent.

Conclusions

The three muscles studied represent a well-defined range of different fibre type populations and have provided a unique opportunity to determine the relationship between fibre type proportions and the characteristics of myoelectric signals quantified by wavelet analysis and principal component analysis. The results show that the level of detail possible from these analyses provides greater insight into the electrophysiology of muscle function than has been commonly reported to date. The differences in motor unit recruitment found across the time course of a stride and the finding that motor unit recruitment does not always hold true to the predictions of the size principle highlight the need for more sensitive methods of analysis to be applied. Optimising signal analysis to high- and low-frequency bands provided a useful way of visualising the interplay between different types of motor unit. This was shown to reconstruct a large proportion of the whole signal, with high- and low-frequency bands being significantly associated with populations of predominantly fast and slow fibre types, respectively. There is growing evidence that current understanding of motor control is limited. Further application of the techniques described here could lead to new understanding of the factors that affect recruitment patterns of motor units and hence provide new insight into motor control.

We thank Michael Boyd and John Thurlbourn for their assistance with the surgical protocol and care of the animals, Dr Alan Wilson for the use of laboratory equipment and Karin Jespers and Pattama Ritruechai for their help with data collection.

References

Adrian, R. H. and Peachey, L. D. (1965). The membrane capacity of frog twitch and slow muscle fibres. *J. Physiol.* **181**, 324-336.

Albuquerque, E. X. and Thesleff, S. (1968). A comparative study of membrane properties of innervated and chronically denervated fast and slow skeletal muscles of the rat. *Acta Physiol. Scand.* **73**, 471-480.

Allison, G. T. and Fujiwara, T. (2002). The relationship between EMG median frequency and low frequency band amplitude changes at different levels of muscle capacity. *Clin. Biomech. Bristol Avon* **17**, 464-469.

Armstrong, R. B. and Phelps, R. O. (1984). Muscle fiber type composition of the rat hindlimb. *Am. J. Anat.* **171**, 259-272.

Bai, T. R., Rabinovitch, B. J. and Pardy, R. L. (1984). Near-maximal voluntary hyperpnea and ventilatory muscle function. *J. Appl. Physiol.* **57**, 1742-1748.

Bottinelli, R., Schiaffino, S. and Reggiani, C. (1991). Force-velocity relations and myosin heavy chain isoform compositions of skinned fibres from rat skeletal muscle. *J. Physiol.* **437**, 655-672.

Bottinelli, R., Betto, R., Schiaffino, S. and Reggiani, C. (1994). Unloaded shortening velocity and myosin heavy chain and alkali light chain isoform composition in rat skeletal muscle fibres. *J. Physiol.* **478**, 341-349.

Brody, L. R., Pollock, M. T., Roy, S. H., De Luca, C. J. and Celli, B. (1991). pH-induced effects on median frequency and conduction velocity of the myoelectric signal. *J. Appl. Physiol.* **71**, 1878-1885.

Burke, R. E., Levine, D. N., Tsairis, P. and Zajac, F. E., 3rd (1973). Physiological types and histochemical profiles in motor units of the cat gastrocnemius. *J. Physiol.* **234**, 723-748.

Caiozzo, V. J., Herrick, R. E. and Baldwin, K. M. (1992). Response of slow and fast muscle to hypothyroidism: maximal shortening velocity and myosin isoforms. *Am. J. Physiol.* **263**, C86-C94.

Calude, C. S. and Stay, M. A. (1995). From Heisenberg to Godel via Chaitin. *Int. J. Theor. Phys.* **44**, 1053-1065.

Daley, M. A. and Biewener, A. A. (2003). Muscle force–length dynamics during level versus incline locomotion: a comparison of *in vivo* performance of two guinea fowl ankle extensors. *J. Exp. Biol.* **206**, 2941-2958.

De Ruiter, C. J., de Haan, A. and Sargeant, A. J. (1995). Physiological characteristics of two extreme muscle compartments in the medial gastrocnemius muscle of the rat. *Acta Physiol. Scand.* **153**, 313-324.

DeLuca, C. J. (1997). The use of surface electromyography in biomechanics. *J. Appl. Biomech.* **13**, 135-136.

Doud, J. R. and Walsh, J. M. (1995). Muscle fatigue and muscle length interaction: effect on the EMG frequency components. *Electromyogr. Clin. Neurophysiol.* **35**, 331-339.

Elert, J. E., Rantapaa-Dahlqvist, S. B., Henriksson-Larsen, K., Lorentzon, R. and Gerdle, B. U. (1992). Muscle performance, electromyography and fibre type composition in fibromyalgia and work-related myalgia. *Scand. J. Rheumatol.* **21**, 28-34.

Esau, S. A., Bellemare, F., Grassino, A., Permutt, S., Roussos, C. and Pardy, R. L. (1983). Changes in relaxation rate with diaphragmatic fatigue in humans. *J. Appl. Physiol.* **54**, 1353-1360.

Gabaldon, A. M., Nelson, F. E. and Roberts, T. J. (2004). Mechanical function of two ankle extensors in wild turkeys: shifts from energy production to energy absorption during incline *versus* decline running. *J. Exp. Biol.* **207**, 2277-2288.

Gallagher, C. G., Hof, V. I. and Younes, M. (1985). Effect of inspiratory muscle fatigue on breathing pattern. *J. Appl. Physiol.* **59**, 1152-1158.

Gerdle, B., Wretling, M. L. and Henriksson-Larsen, K. (1988). Do the fibre-type proportion and the angular velocity influence the mean power frequency of the electromyogram? *Acta Physiol. Scand.* **134**, 341-346.

Gillespie, C. A., Simpson, D. R. and Edgerton, V. R. (1974). Motor unit recruitment as reflected by muscle fibre glycogen loss in a prosimian (bushbaby) after running and jumping. *J. Neurol. Neurosurg. Psychiatr.* **37**, 817-824.

Gillis, G. B. and Biewener, A. A. (2001). Hindlimb muscle function in relation to speed and gait: *in vivo* patterns of strain and activation in a hip and knee extensor of the rat (*Rattus norvegicus*). *J. Exp. Biol.* **204**, 2717-2731.

Gillis, G. B. and Biewener, A. A. (2002). Effects of surface grade on proximal hindlimb muscle strain and activation during rat locomotion. *J. Appl. Physiol.* **93**, 1731-1743.

Gollnick, P. D., Piehl, K. and Saltin, B. (1974). Selective glycogen depletion pattern in human muscle fibres after exercise of varying intensity and at varying pedalling rates. *J. Physiol.* **241**, 45-57.

Grimby, L. and Hannerz, J. (1977). Firing rate and recruitment order of toe extensor motor units in different modes of voluntary conraction. *J. Physiol.* **264**, 865-879.

He, Z.-H., Bottinelli, R., Pellegrino, M. A., Ferenczi, M. A. and Reggiani, C. (2000). ATP consumption and efficiency of human single muscle fibers with different myosin isoform composition. *Biophys. J.* **79**, 945-961.

Henneman, E. and Olson, C. B. (1965). Relations between structure and function in the design of skeletal muscles. *J. Neurophysiol.* **28**, 581-598.

Henneman, E., Somjen, G. and Carpenter, D. O. (1965a). Excitability and inhibitability of motoneurons of different sizes. *J. Neurophysiol.* **28**, 599-620.

Henneman, E., Somjen, G. and Carpenter, D. O. (1965b). Functional significance of cell size in spinal motoneurons. *J. Neurophysiol.* **28**, 560-580.

Hill, A. V. (1950). The dimensions of animals and their muscular dynamics. *Sci. Prog.* **38**, 209-230.

Hoffer, J. A., O'Donovan, M. J., Pratt, C. A. and Loeb, G. E. (1981). Discharge patterns of hindlimb motoneurons during normal cat locomotion. *Science* **213**, 466-467.

Jayne, B. C. and Lauder, G. V. (1994). How swimming fish use slow and fast muscle fibers: implications for models of vertebrate muscle recruitment. *J. Comp. Physiol. A* **175**, 123-131.

Johnston, I. (1991). Muscle action during locomotion: a comparative perspective. *J. Exp. Biol.* **160**, 167-185.
Kaiser, G. (1994). *A Friendly Guide to Wavelets*. Boston, Basel, Berlin: Birkhäuser.
Kanda, K., Burke, R. E. and Walmsley, B. (1977). Differential control of fast and slow twitch motor units in the decerebrate cat. *Exp. Brain Res.* **29**, 57-74.
Loeb, G. E. (1985). Motoneurone task groups: coping with kinematic heterogeneity. *J. Exp. Biol.* **115**, 137-146.
Loeb, G. E. and Gans, C. (1986). *Electromyography for Experimentalists*. Chicago: University of Chicago Press.
Luff, A. R. and Atwood, H. L. (1972). Membrane properties and contraction of single muscle fibers in the mouse. *Am. J. Physiol.* **222**, 1435-1440.
Mallat, S. G. (1998). *A Wavelet Tour of Signal Processing*. San Diego, London, Boston, New York, Sydney, Tokyo, Toronto: Academic Press.
Mundermann, A., Wakeling, J. M., Nigg, B. M., Humble, R. N. and Stefanyshyn, D. J. (2006). Foot orthoses affect frequency components of muscle activity in the lower extremity. *Gait Posture* **23**, 295-302.
Nardone, A., Romano, C. and Schieppati, M. (1989). Selective recruitment of high-threshold human motor units during voluntary isotonic lengthening of active muscles. *J. Physiol.* **409**, 451-471.
Peter, J. B., Barnard, R. J., Edgerton, V. R., Gillespie, C. A. and Stempel, K. E. (1972). Metabolic profiles of three fiber types of skeletal muscle in guinea pigs and rabbits. *Biochemistry* **11**, 2627-2633.
Petrofsky, J. S. (1979). Frequency and amplitude analysis of the EMG during exercise on the bicycle ergometer. *Eur. J. Appl. Physiol. Occup. Physiol.* **41**, 1-15.
Prilutsky, B., Herzog, W. and Allinger, T. (1996). Mechanical power and work of cat soleus, gastrocnemius and plantaris muscles during locomotion: possible functional significance of muscle design and force patterns. *J. Exp. Biol.* **199**, 801-814.
Ramsay, J. O. and Silverman, B. W. (1997). *Functional Data Analysis*. New York: Springer.
Rome, L. C., Funke, R. P., Alexander, R. M., Lutz, G. J., Aldridge, H., Scott, F. and Freadman, M. (1988). Why animals have different muscle fibre types. *Nature* **335**, 824-827.
Schiaffino, S. and Reggiani, C. (1994). Myosin isoforms in mammalian skeletal muscle. *J. Appl. Physiol.* **77**, 493-501.
Schiaffino, S., Gorza, L., Sartore, S., Saggin, L., Ausoni, S., Vianello, M., Gundersen, K. and Lomo, T. (1989). Three myosin heavy chain isoforms in type 2 skeletal muscle fibres. *J. Muscle Res. Cell Motil.* **10**, 197-205.
Smith, J. L., Betts, B., Edgerton, V. R. and Zernicke, R. F. (1980). Rapid ankle extension during paw shakes: selective recruitment of fast ankle extensors. *J. Neurophysiol.* **43**, 612-620.
Stalberg, E. (1966). Propagation velocity in human muscle fibers in situ. *Acta Physiol. Scand. Suppl.* **287**, 1-112.
Stanfield, P. R. (1972). Electrical properties of white and red muscle fibres of the elasmobranch fish *Scyliorhinus canicula*. *J. Physiol.* **222**, 161-186.
Swoap, S. J., Caiozzo, V. J. and Baldwin, K. M. (1997). Optimal shortening velocities for in situ power production of rat soleus and plantaris muscles. *Am. J. Physiol.* **273**, C1057-C1063.
von Tscharner, V. (2000). Intensity analysis in time-frequency space of surface myoelectric signals by wavelets of specified resolution. *J. Electromyogr. Kinesiol.* **10**, 433-445.
von Tscharner, V. (2002). Time-frequency and principal-component methods for the analysis of EMGs recorded during a mildly fatiguing exercise on a cycle ergometer. *J. Electromyogr. Kinesiol.* **12**, 479-492.
Von Tscharner, V. and Goepfert, B. (2006). Estimation of the interplay between groups of fast and slow muscle fibers of the tibialis anterior and gastrocnemius muscle while running. *J. Electromyogr. Kinesiol.* **16**, 188-197.
Wakeling, J. M. (2004). Motor units are recruited in a task-dependent fashion during locomotion. *J. Exp. Biol.* **207**, 3883-3890.
Wakeling, J. M. (2005). Motor unit recruitment during vertebrate locomotion. *Anim. Biol.* **55**, 41-58.
Wakeling, J. M. and Rozitis, A. I. (2004). Spectral properties of myoelectric signals from different motor units in the leg extensor muscles. *J. Exp. Biol.* **207**, 2519-2528.
Wakeling, J. M. and Syme, D. A. (2002). Wave properties of action potentials from fast and slow motor units of rats. *Muscle Nerve* **26**, 659-668.
Wakeling, J. M., Pascual, S. A., Nigg, B. M. and Von Tscharner, V. (2001a). Surface EMG shows distinct populations of muscle activity when measured during sustained sub-maximal exercise. *Eur. J. Appl. Physiol.* **86**, 40-47.
Wakeling, J. M., Von Tscharner, V., Nigg, B. M. and Stergiou, P. (2001b). Muscle activity in the leg is tuned in response to ground reaction forces. *J. Appl. Physiol.* **91**, 1307-1317.
Wakeling, J. M., Kaya, M., Temple, G. K., Johnston, I. A. and Herzog, W. (2002). Determining patterns of motor recruitment during locomotion. *J. Exp. Biol.* **205**, 359-369.
Wakeling, J. M., Uehli, K. and Rozitis, A. I. (2006). Muscle fibre recruitment can respond to the mechanics of the muscle contraction. *J. R. Soc. Interface* **3**, 533-544.